Probing the local structure of pure ionic liquid salts with solid- and liquid-state NMR

Gordon, Peter G.; Brouwer, Darren H.; Ripmeester, John A.

Publisher's version / Version de l'éditeur:
https://doi.org/10.1002/cphc.200900624
ChemPhysChem, 11, 1, pp. 260-268, 2010-01-18

CHEMPHYSCHEM

DOI: 10.1002/cphc.200900624

Probing the Local Structure of Pure Ionic Liquid Salts with Solid- and Liquid-State NMR**

Peter G. Gordon,[a, b] Darren H. Brouwer,[a] and John A. Ripmeester*[a]

Room-temperature ionic liquids (RTILs) are gaining increasing interest and are considered part of the green chemistry paradigm due to their negligible vapour pressure and ease of recycling. Evidence of liquid-state order, observed by IR and Raman spectroscopy, diffraction studies, and simulated by ab initio methods, has been reported in the literature. Here, quadrupolar nuclei are used as NMR probes to extract information about the solid and possible residual order in the liquid state of RTILs. To this end, the anisotropic nature and field dependence of quadrupolar and chemical shift interactions are exploited. Relaxation time measurements and a search for residual second-order quadrupolar coupling were employed to investigate the molecular motions present in the liquid state and infer what kind of order is present. The results obtained indicate that on a timescale of $\sim 10^{-8}$ sec or longer, RTILs behave as isotropic liquids without residual order.

1. Introduction

Ionic liquids (ILs) have been known for nearly a century[1] but initially there was little interest in investigating their use as solvents. The term "room-temperature ionic liquids" (RTILs) is often used interchangeably with "ionic liquids" and is loosely defined as those ILs that have melting points at around or below 100 °C. Their low volatility has made them attractive targets as substitutes for volatile organic solvents. A broad spectrum of tunable properties arises from the customizability of the organic cation and the variety of cation–anion pairings and so ILs are often denoted as "designer solvents". Ionic liquids are finding uses as solvents and reaction media in a large number of diverse applications such as carbon dioxide sensors,[2] catalysis,[3,4] energy storage,[5] nanostructure synthesis,[6,7] and many others.

Due to the enormous number of potential cation–anion combinations, it is impossible to investigate directly even a small fraction of the set of feasible ILs. Thus, to develop a molecular understanding of their properties requires generalizations from representative systems. Of primary concern and controversy is the nature of the liquid state, in particular the type and extent of molecular order present. Theories, and experimental support, range from simple ion pairs to liquid-crystal-type order depending on the characterization technique employed, the IL under study, and the interpretation of the data. It appears that only two clear trends can be distinguished that result in increased order in the liquid state: increased alkyl substituent length on the cation, and smaller anions. Furthermore, even where there is agreement with regards to the presence of some kind of nanostructure, its nature is not yet fully agreed upon. For example, early studies led the investigators to report extended hydrogen-bonding networks, but subsequent research has suggested that the type of bonding observed is not entirely consistent with the hydrogen-bonding model.[8]

The present work describes an investigation into the environment of IL halide counterions in the solid and liquid states by quadrupolar nuclear magnetic resonance (NMR) spectroscopy. Resolving the field-dependent spectral features of the solid-state samples at lower fields remains a challenge and so high-field spectra, both magic-angle spinning (MAS) and static, were used to determine both quadrupolar and chemical shift parameters. Subtle changes in the electronic (and magnetic) environment of a quadrupolar nucleus are readily observed by NMR and this work builds upon previously published solid-state investigations of chloride ILs.[9] Scheme 1 shows the structures of the cations described herein along with their abbreviations.

2. Theoretical Background

Here we briefly review some relevant concepts, terminology and conventions pertaining to solid-state NMR (SSNMR) of quadrupolar halogens. It is the quadrupolar nature of these nuclei that afford a probe into their surroundings in both the solid and liquid states.

[a] P. G. Gordon, Dr. D. H. Brouwer, Dr. J. A. Ripmeester
National Research Council
Steacie Institute for Molecular Sciences
100 Sussex Ave., Ottawa, ON, K1A 0R6 (Canada)
Fax: (+1) 613-998-7833
E-mail: John.Ripmeester@nrc-cnrc.gc.ca

[b] P. G. Gordon
Department of Chemistry
Carleton University
1125 Colonel By Drive, Ottawa, ON, K1S 5B6 (Canada)

[**] ^{35}Cl, ^{79}Br and ^{127}I Solid- and Liquid-State NMR

Supporting information for this article is available on the WWW under http://dx.doi.org/10.1002/cphc.200900624.

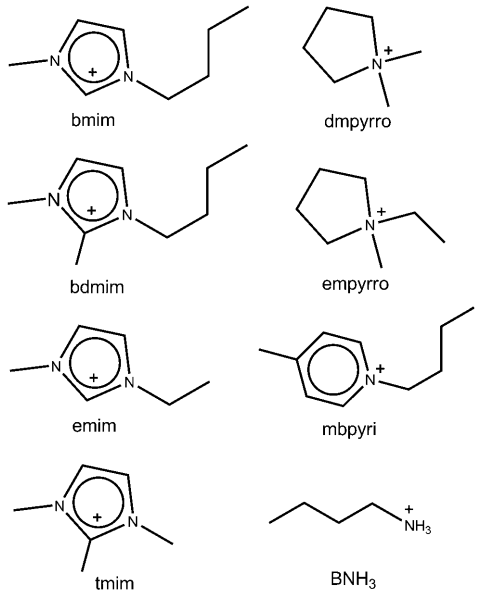

Scheme 1. Structures of the cations described herein and their abbreviations.

2.1. The Nuclear Electric Quadrupole Interaction

The quadrupole interaction Hamiltonian describing the interaction between the nuclear electric quadrupole moment of a nucleus of spin I and an electric field gradient V is given by Equation (1) in angular frequency units:

$$\hat{H}_Q = \frac{eQ}{2I(2I-1)\hbar}\hat{I}V\hat{I} \tag{1}$$

The electric field gradient (EFG) can be represented by a second-rank tensor and described by the nuclear quadrupolar coupling constant, C_Q, given by Equation (2):

$$C_Q = \frac{eV_{33}Q}{h} \tag{2}$$

and by the asymmetry parameter, η_Q, given by Equation (3):

$$\eta_Q = \frac{V_{11}-V_{22}}{V_{33}} \tag{3}$$

where the principal components of the diagonalized EFG tensor are arraged as $|V_{33}| \geq |V_{22}| \geq |V_{11}|$ and e is the charge of an electron.

2.2. The Nuclear Magnetic Shielding Interaction

The chemical shielding (CS) Hamiltonian acting on a spin I is given by Equation (4), in frequency units:

$$\hat{H}_{CS} = \gamma\hat{I}\sigma B_0 \tag{4}$$

The second-rank tensor σ, called the chemical shielding tensor, is used to describe the extent of the shielding and its dependence on molecular orientation. The axis frame of this tensor, called the principal axis frame, is chosen such that the tensor is diagonal. The principal values of the shielding tensor are seldom given; often a set of quantities based on these values is given instead to provide a more intuitive representation of the strength of the interaction and its orientation dependence. Herein, these are expressed (using the Herzfeld–Berger convention) as the isotropic value δ_{iso}, the span Ω and the skew κ, as in Equation (5):

$$\begin{aligned}\delta_{iso} &= \sigma_{ref} - \frac{\sigma_{11}+\sigma_{22}+\sigma_{33}}{3}\\ \Omega &= \sigma_{33}-\sigma_{11}\\ \kappa &= \frac{3(\sigma_{22}-\sigma_{iso})}{\Omega}\end{aligned} \tag{5}$$

where σ_{11}, σ_{22} and σ_{33} are the principal values of the shielding tensor. In a simple spectrum the components of the tensor can be determined experimentally from chemical shift powder patterns and in more complicated spectra (where multiple sites and/or interactions are present) the components can be determined experimentally from a collected spectrum by way of a simulation calculated to reproduce the lineshape, as with the quadrupolar interaction.

2.3. The Central Transition

With a significant quadrupolar interaction corrections must be made to the energies of the Zeeman levels, as the interaction results in additional splitting. For splitting of less than ~1/10 of the Zeeman splitting, first- and second-order corrections are sufficient, given by Equation (6):

$$\begin{aligned}E_m^{(1)} &= \frac{e^2qQ}{4I(2I-1)}[3m^2-I(I+1)]\frac{1}{2}(3\cos^2\theta-1+\eta\cos 2\phi\sin^2\theta)\\ E_m^{(2)} &= -\left[\frac{e^2qQ}{4I(2I-1)}\right]^2\frac{m}{\omega_o}\left\{-\frac{1}{5}[I(I+1)-3m^2](3+\eta_Q^2)\right.\\ &+\frac{1}{28}[8I(I+1)-12m^2-3][(\eta_Q^2-3)(3\cos^2\theta-1)+6\eta_Q\sin^2\theta\cos 2\phi]\\ &+\frac{1}{8}[18I(I+1)-34m^2-5]\left[\frac{1}{140}(18+\eta^2)(35\cos^4\theta-30\cos^2\theta+3)\right.\\ &\left.\left.+\frac{3}{7}\eta_Q\sin^2\theta(7\cos^2\theta-1)\cos 2\phi+\frac{1}{4}\eta_Q^2\sin^4\theta\cos 4\phi\right]\right\}\end{aligned} \tag{6}$$

where m denotes the magnetic quantum number associated with that particular Zeeman level and θ and ϕ are polar angles which define the orientation of B_o in the principal axis system of the EFG tensor.

In the context of the present work, it is important to note that the first term of the second-order energy correction is isotropic. The result is that the isotropic shift for a quadrupolar nucleus has a contribution from both the quadrupolar coupling and the chemical shift interaction. This allows the quadrupolar interaction to be diagnostic of local order in the liquid phase. If there is no local order that persists on a timescale of

the motional correlation time at the relaxation time minimum $\tau_c \sim 1/\omega_o$, then there will be no residual quadrupolar interaction and the isotropic shift will be invariant at different magnetic field strengths. In the presence of a residual quadrupole interaction, the apparent chemical shift (δ_{obs}) will vary with the magnetic field according to Equation (7):

$$\delta_{obs} - \delta_{iso} \propto \left(\frac{C_Q}{\upsilon_o}\right)^2 \quad (7)$$

where υ_o is the nuclear resonance frequency.[10]

2.4. NMR Tensor Conventions

The principal axes of the tensors that describe the chemical shift and quadrupolar interactions are often not coincident and so their relative orientation must be considered. This is described by the set of rotations required to obtain the proper relative orientation of the axes of the tensors, in terms of the Euler angles α, β and γ. Herein we use the same convention as Mehring.[11]

The spectra reported herein show only the central ($-1/2$ to $+1/2$) transition. This transition is affected by the second-order quadrupolar coupling as well as the chemical shift interaction and is sensitive to the angles between the two tensors[12] and so carries all information of interest to this investigation. Chemical shift and second-order quadrupolar couplings have opposite magnetic field dependencies and so spectra obtained at different fields have been acquired, offering a good confirmation of the parameters determined via simulation.

3. Results and Discussion

3.1. Chloride ILs

The ^{35}Cl SSNMR spectra for the chloride salts, experimental and simulated, are shown in Figure 1. Experimentally determined quadrupolar and CS tensor parameters obtained by simulation of the acquired spectra are listed in Table 1. Isotropic chemical shifts are reported relative to 0.1 M NaCl in D_2O.

The number of sites observed in each sample correspond to the crystal structures available for emim, bmim and bdmim[Cl][13–17] and obtained by X-ray diffraction for mbpyr[Cl].[18] A complete set of CS tensor parameters and angles between tensors were found for the single-site samples; the multiple-site samples proved difficult to characterize satisfactorily due to overlapping lineshapes.

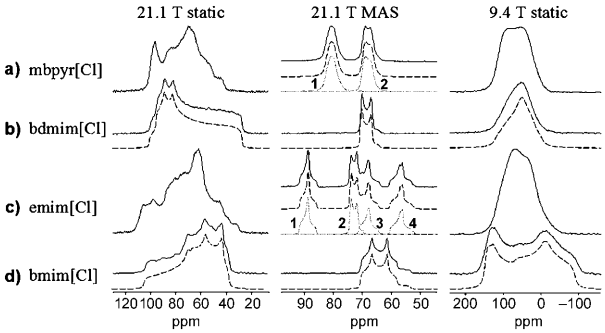

Figure 1. Chloride IL ^{35}Cl spectra of powdered samples. a) ethyl-methyl-pyridinium, b) butyl-dimethyl-imidazolium, c) ethyl-methyl-imidazolium, d) butyl-methyl-imidazolium with static spectra at 21.15 T (left), MAS spectra at 21.15 T (center) and static spectra at 9.39 T (right). (----): Best-fit calculated spectra with parameters listed in Table 1. Labeled peaks denote corresponding table values. MAS rate = 10 kHz.

The quadrupolar coupling constants range from 0.8 to 1.5 MHz and quadrupolar asymmetry parameters range from 0 to 0.95. Typical C_Q values for chloride ions in organic and inorganic salts range from zero to greater than 9.0 MHz.[19–22] The CS tensor values are consistent with those found in other organic-chloride systems; Wasylishen reported δ_{iso} of 10–53 ppm for a series of five organic hydrochlorides[23] and Chapman reported 37–120 ppm for another series of ten organic hydrochlorides.[19] Here, a relatively narrow range of 61–92 ppm was observed. Spans in the same studies report a range of 45–150 ppm; spans of 44 and 78 ppm are reported here. These studies by Wasylishen and Bryce concerned hydrogen-bonded chlorides, and hydrogen bonding is generally regarded as an important interaction governing the structure and behaviour of imidazolium ionic liquids.[13–15] At least one ab initio study has been performed in which the authors conclude that the bonding is "considerably different from that of conventional hydrogen bonds".[24] That being said, the Cl–H distances involved are similar to values typical of hydrogen bonding.

Table 1. ^{35}Cl experimental spectrum simulation fit parameters.

Cation[a]		C_Q [MHz]	η_Q	δ_{iso} [ppm]	Ω [ppm]	κ	α [°][b]	β [°]	γ [°]
mbpyri	1	0.857 ± 0.008	0.525 ± 0.005	83.15 ± 0.07	–	–	–	–	–
	2	0.889 ± 0.008	0.08 ± 0.08	70.56 ± 0.04	–	–	–	–	–
bmmim		0.978 ± 0.004	0.10 ± 0.02	71.60 ± 0.02	−47.4 ± 0.2	0.28 ± 0.01	16 ± 1	82.5 ± 0.5	−34 ± 4
emim	1	0.808 ± 0.004	0.95 ± 0.01	91.72 ± 0.03	–	–	–	–	–
	2	0.805 ± 0.005	0.20 ± 0.02	74.98 ± 0.04	–	–	–	–	–
	3	0.884 ± 0.004	0.86 ± 0.01	71.36 ± 0.04	–	–	–	–	–
	4	0.972 ± 0.005	0.80 ± 0.01	60.60 ± 0.03	–	–	–	–	–
bmim		1.500 ± 0.002	0.390 ± 0.005	71.65 ± 0.05	25.0 ± 0.5	0.48 ± 0.04	78 ± 2	76 ± 1	12 ± 2

[a] See Scheme 1 for the structures and abbreviations of the cations used herein. [b] Euler angles use the ZYZ convention. Quadrupolar parameter errors estimated using MAS 21.15 T spectra, CSA parameter errors estimated using static 21.15 T spectra. Labeled parameters correspond to their respective peaks in Figure 1. Isotropic chemical shifts are reported relative to 0.1 M NaCl in D_2O.

3.2. Bromide ILs

The ^{79}Br SSNMR spectra for the bromide salts, experimental and simulated, are shown in Figure 2. Experimentally determined quadrupolar and CS tensor parameters obtained by simulation of the acquired spectra are listed in Table 2. Isotropic chemical shifts are reported relative to 0.01 M NaBr in D_2O.

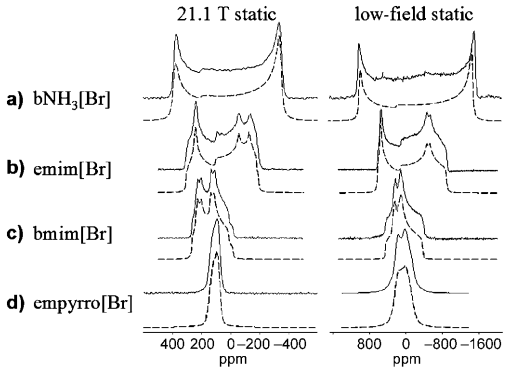

Figure 2. Bromide IL ^{79}Br spectra of powdered samples. (——): Experimental. (-----): Simulated.

The ^{79}Br quadrupolar coupling constants cover a relatively large range, from 5.1 to 17.5 MHz, and quadrupolar asymmetry parameters range from zero to 0.86. There are far fewer SSNMR studies available for organic bromide systems than for organic chlorides, making comparisons difficult. The relatively large nuclear electric quadrupole moment of ^{79}Br leads to very large linewidths in systems that do not possess high symmetry and so most research has been restricted to high symmetry inorganic solids. The results obtained herein are not out of line with those presented in a review of bromine-79/81 SSNMR.[25] The number of sites observed in emim and bmim[Br] correspond to the crystal structures reported in the literature.[13,14]

3.3. Iodide ILs

The ^{127}I SSNMR spectra for the iodide salts, experimental and simulated, are shown in Figure 3. Experimentally determined quadrupolar and CS tensor parameters obtained by simulation of the acquired spectra are listed in Table 3. Isotropic chemical shifts are reported relative to 0.01 M KI in D_2O.

Only two iodide sample spectra were amenable to simulation, yielding quadrupolar constants of 17 MHz and 37 MHz

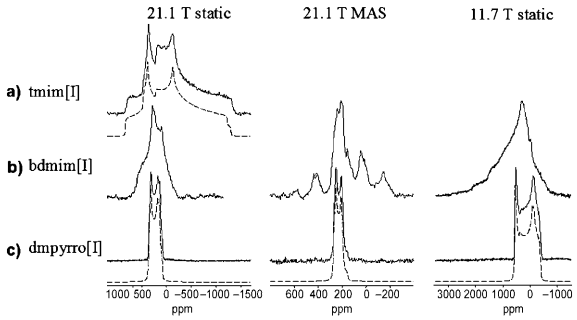

Figure 3. Iodide IL ^{127}I spectra of powdered samples. (——): Experimental. (-----): Simulated.

and asymmetry parameters of 0.27 and 0.73. As with organic bromides, there are very few organic iodide SSNMR studies available for comparison. Again, the parameter values reported herein are in line with those few presented in Bryce's review.[25] No crystal structures were available for these ILs. The spectra for bdmim[I] suggest the presence of more than one site, however the signal was too broad to fully "spin out" the interactions and as a result spinning side-bands frustrated efforts to clarify the spectrum and extract parameters.

3.4. Liquid-State NMR

Chloride ILs

The liquid-state NMR spectra for the chloride samples are presented in Figure 4. Simple isotropic lineshapes were observed. Spectra were acquired at two field strengths, 9.4 T and 4.7 T, to test for the presence of second-order quadrupolar effects which would indicate the presence of some persistent order. No significant differences, either in isotropic shift or in linewidth, were observed.

The transition from the solid to liquid state was observed by stepwise variable-temperature NMR (VTNMR). The temperature was increased from room temperature and held at the target temperature for at least ten minutes prior to acquisition to allow the sample ample time to equilibrate. Acquisition times were of the order of 30 min.

The progression from solid to liquid state is illustrated in Figures 5, 6 and 7 for emim, bmim and bdmim[Cl] respectively; the spectra are aligned with the appropriate region in the differential scanning calorometry (DSC) trace of the sample.

Table 2. ^{79}Br experimental spectrum simulation fit parameters.

Cation[a]	C_Q [MHz]	η	δ_{iso} [ppm]	Ω [ppm]	κ	α [°][b]	β [°]	γ [°]
bNH_3	17.50 ± 0.02	0.01 ± 0.01	137.0 ± 0.5	75 ± 2	0.05 ± 0.05	0	0	0
emim	12.40 ± 0.01	0.28 ± 0.01	122 ± 1	73 ± 3	0.95 ± 0.05	54 ± 3	81 ± 1	8 ± 2
bmim	7.35 ± 0.05	0.86 ± 0.02	172 ± 1	−58 ± 2	0.64 ± 0.10	108 ± 3	18 ± 3	57 ± 3
empyrro	5.12 ± 0.05	0.37 ± 0.08	123 ± 1	51 ± 1	0.96 ± 0.04	-83 ± 2	−21 ± 2	148 ± 2

[a] See Scheme 1 for the structures and abbreviations of the cations used herein. [b] Euler angles use the ZYZ convention. Quadrupolar parameter errors estimated using MAS 21.15 T spectra, CSA parameter errors estimated using static 21.15 T spectra. Isotropic chemical shifts are reported relative to 0.01 M NaBr in D_2O.

Table 3. ^{127}I experimental spectrum simulation fit parameters.

Cation[a]	C_Q [MHz]	η	δ_{iso} [ppm]	Ω [ppm]	κ	α [°][b]	β [°]	γ [°]
trimim	36.8 ± 0.9	0.73 ± 0.01	143 ± 18	0	0	–	–	–
mmpyrro	16.9 ± 0.1	0.27 ± 0.02	282.0 ± 0.7	184 ± 3	−0.20 ± 0.05	56 ± 7	13 ± 2	31 ± 5

[a] See Scheme 1 for the structures and abbreviations of the cations used herein. [b] Euler angles use the ZYZ convention. Quadrupolar parameter errors estimated using MAS 21.15 T spectra, CSA parameter errors estimated using static 21.15 T spectra. Isotropic chemical shifts are reported relative to 0.01 M KI in D_2O.

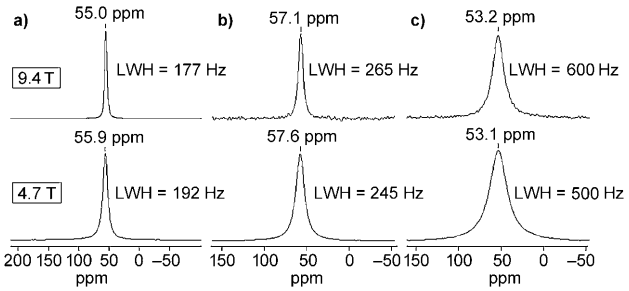

Figure 4. Liquid-state ^{35}Cl spectra. a) emim, b) bmim, c) bdmim chlorides.

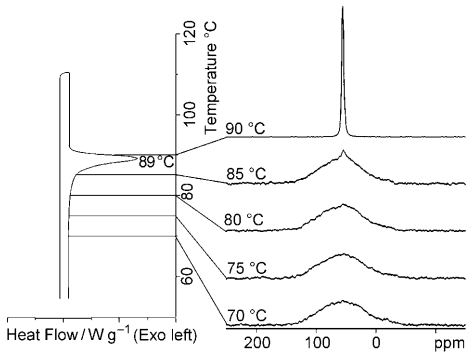

Figure 5. DSC profile with ^{35}Cl NMR spectra at 9.4 T for emim[Cl]

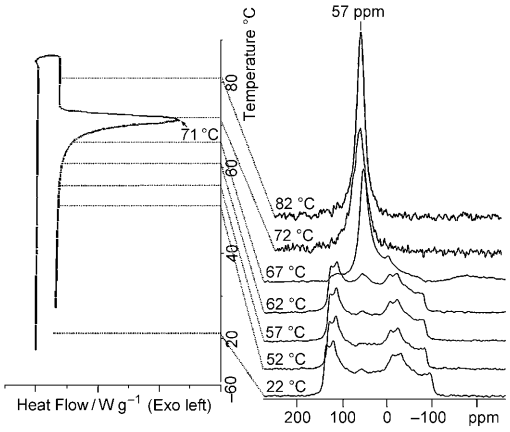

Figure 6. DSC profile with ^{35}Cl NMR spectra at 9.4 T for bmim[Cl]

These traces were acquired at 1 °C min^{-1} separately from the NMR spectra and it must be emphasized that the trace is only meant as a guide for experiment and not an exact correlation.

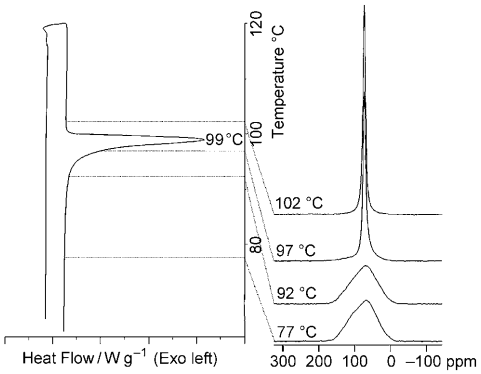

Figure 7. DSC profile with ^{35}Cl NMR spectra at 9.4 T for bdmim[Cl]

Examination of the spectra for emim and bmim[Cl] show evidence of partial melting prior to observation of isotropic peaks; the isotropic peak can be seen "growing" out of the solid lineshape. The spectra for bdmim[Cl] show a sharp transition from solid lineshape to isotropic liquid peak over a 5 °C increase. In each series the solid lineshape is observed to disappear abruptly and entirely.

Figure 8 stacks the liquid state ^{35}Cl spectra acquired from a bmim[Cl] sample as it was cooled. The temperature ramping employed followed the procedure reported by Hayashi and coworkers in their Raman work.[16] They reported an increase in the intensity of Raman bands attributed to a specific conformation of the bmim cation, concluding that some local struc-

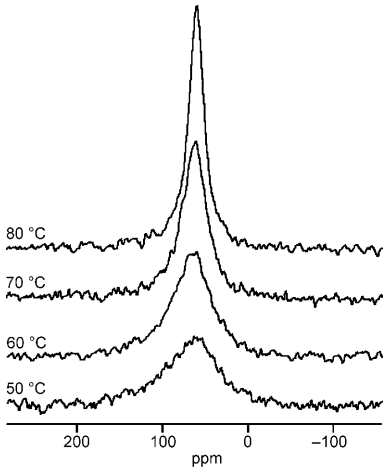

Figure 8. ^{35}Cl VTNMR at 9.4 T of bmim[Cl], cooled from 80 °C to 50 °C

ture exists in the liquid state. The NMR spectra reported herein show line broadening with decreased temperature and a decrease in signal strength. Both of these are expected as a sample is cooled and viscosity increases, but neither observation provides support for local structure that persists on correlation times longer than $\tau_c \sim 1/\omega_o$. Of course, other techniques have their own associated time scales for providing evidence for local structure.

Bromide ILs

The liquid-state NMR spectra for two bromide samples, emim and bmim[Br], are presented in Figure 9. The molten spectrum of bNH_3[Br] was not acquired due to moisture contamination of the sample and time constraints. Results comparable to those obtained for the chloride samples were observed. As for the other samples, the ^{79}Br signal from molten bdmim[Br] was not seen and is speculated to be too broad to be acquired, and the melting temperature of mbpyr[Br] was not obtainable with the available VTNMR apparatus. Simple isotropic lineshapes were again observed. As with the chlorides, spectra were acquired at two field strengths, 9.4 T and 4.7 T to test for the presence of second-order quadrupolar effects. No significant difference, either in isotropic shift or in linewidth was observed for emim[Br]. The spectra collected from liquid bmim[Br] samples do appear to show some significant differences in both isotropic shift and linewidth. However the shift observed is opposite in direction to that expected from second-order quadrupolar interaction effects. It is proposed that the differences seen here stem from approaching the experimental limits of the equipment used; the breadth of the sweep width necessary to acquire the spectrum at 4.7 T introduced distortions in the spectrum that rendered accurate phasing problematic. This view is supported by investigations of T_1 and T_2 relaxation times reported below, which support the lack of persistent local structure.

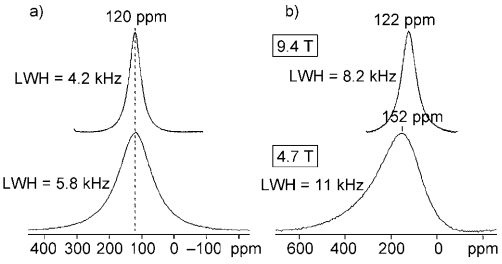

Figure 9. Liquid-state ^{79}Br NMR spectra. a) emim[Br] and b) bmim[Br].

3.5. Relaxation Time Experiments

T_1 and T_2 measurements of molten samples were performed to further probe the nature of the local order, if any, of the ILs. The ratio T_1/T_2 near the melting point of a sample can be diagnostic in this regard: a large ratio results from strong residual interactions indicative of local structure while a ratio of one (1) indicates an isotropic liquid. Intermediate values close to unity are typical of viscous liquids, where the ratio increases with increasing viscosity. Experimental results are illustrated in Figures 10 and 11 for the chlorides and bromides respectively.

As with the VTNMR experiments reported above, samples were allowed to equilibrate at the target temperature for at least ten minutes prior to acquisition. Each sample was heated from 20 to 40 °C above its melting point, and then cooled. In Figure 10a, emim[Cl] is observed to transition from a isotropic liquid to a solid. In the liquid regime the ratio averages 1.88 ± 0.10. For bmim and bdmim[Cl] the solid regime is not included. An average T_1/T_2 ratio of 2.63 ± 0.12 was observed for bmim[Cl], 2.93 ± 0.13 for bdmim[Cl], 1.26 ± 0.13 for emim[Br] and 1.07 ± 0.08 for bmim[Br].

These ratios are all consistent with liquids of relatively low viscosity. In such samples, there are molecular motions that correspond to correlation times on the scale of the inverse Larmor frequency of the nucleus under study (39.2 MHz for ^{35}Cl and 100.2 MHz for ^{79}Br) which reduces the value of T_1, as well as some slightly slower molecular motions which are responsible for a further reduction in the T_2 constant. The observed ratios are not high enough to suggest sustained order in the liquid state.

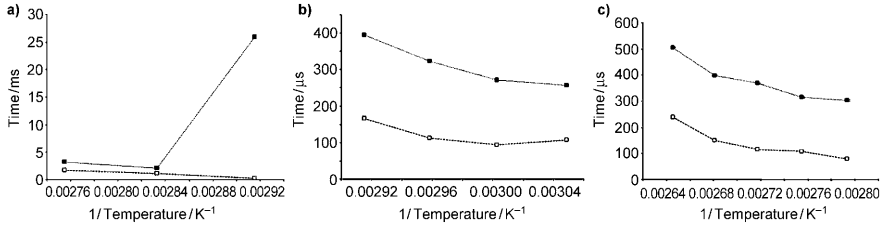

Figure 10. Relaxation times for chloride ILs. a) emim[Cl], b) bmim[Cl], c) bdmim[Cl]. (■): T_1 values. (□): T_2 values.

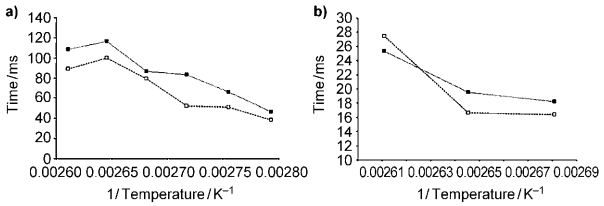

Figure 11. Relaxation times for bromide ILs. **(a)** emim[Br] and **(b)** bmim[Br]. (■): T_1 values. (□): T_2 values.

3.6. Gaussian Calculations

In order to compare experimentally obtained values with theory, ab initio calculations of ^{35}Cl quadrupolar and chemical

shift anisotropy interactions were performed; the heavier anions are not amenable to this method. Proton positions were optimized prior to NMR tensor calculations using the B3LYP method and the 3-21G* basis set. All EFG tensor calculations were done at the restricted Hartree–Fock (RHF) level of theory with the Dunning-type cc-pVTZ basis set for the central chloride ion. The cc-pVDZ basis set was used for all other atoms. Shielding tensor calculations were likewise performed using a hybrid B3LYP DFT method, with a basis set of aug-cc-pVDZ for chlorine and cc-pVDZ for all other atoms. The chlorine EFG and shielding tensors generated in the Gaussian output files were then analyzed using the EFGShield program (version 2.2).[26] The resulting parameters are tabulated along with their experimental counterparts in Table 4.

Reasonable agreement with respect to the quadrupolar coupling constant and isotropic shifts were obtained, with the significant exception of one site in emim[Cl]. The C_Q values of the other IL sites were reproduced within 37%, with an average error of 22%, excluding that of emim[Cl], which the calculation overestimated by 69% (note that experiment cannot determine the sign of C_Q). These errors are slightly higher than those reported using the same basis sets by Chapman and Bryce on organic chloride systems (<12%).[19] Using available crystal structure data, calculations were based on a reduced set of atoms (necessary for timely results); this is likely a significant source of error, as it made unavoidable changes to bonding and hence electron distribution. It would be reasonable to assume that removing nearby chlorides might also have an impact on C_Q calculations however the first two nuclei listed in Table 4 each have a chloride within 5.24 Å and each calculation gives a significantly different error of 9 and 69%. The next largest error (37%) is seen for bmim[Cl], whose smallest Cl–Cl distance is 4.7 Å. A comparison of theoretical and experimental values is illustrated in Figure 12.

Better agreement was obtained between the experimental and calculated isotropic chemical shifts; all were within 27% with an average of 14% deviation. In the same paper mentioned above, Chapman and Bryce reported an underestimation of the isotropic shift in all but one of the systems studied. Herein, five shifts were underestimated and three were overestimated by theory. The obtained values for the chemical shift spans were in good agreement, but with only two experimental values for comparison, a trend cannot be assumed.

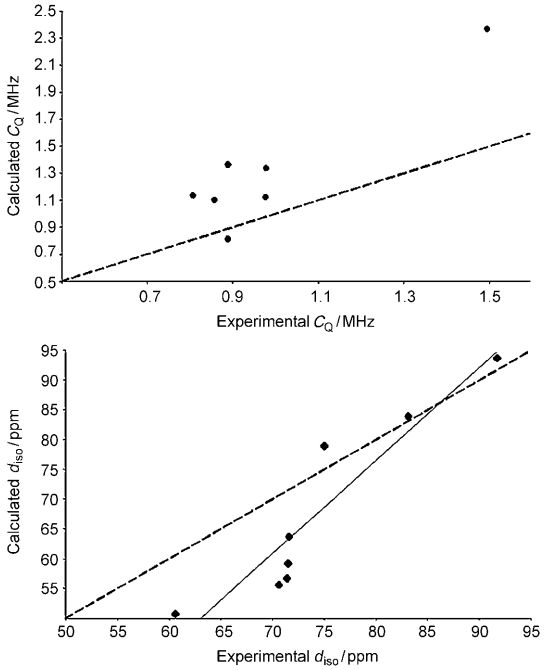

Figure 12. Comparison of experimentally obtained parameters and those calculated with Gaussian 98. (-----): Best-case scenario of Calculated = Experimental. The equation for the line of best fit (—— in right chart) is $y = 1.56x - 48.43$, with an R-value of 0.87.

4. Conclusions

The environment of halides in a selection of ionic liquids was investigated experimentally by NMR spectroscopy and some of the NMR parameters for the solids were calculated as well. It was discovered that for chloride, bromide and iodide ILs in the solid state, the quadrupolar and chemical shift interactions of the halide nucleus are consistent with those found in other solid organic chloride, bromide and iodide salts. Theoretical

Table 4. Experimental ^{35}Cl nuclear quadrupole and CSA parameters with those calculated by Gaussian 98 (G98).

Cation	C_Q *G98* [MHz]	C_Q [MHz]	η *G98*	η	d_{iso} *G98* [ppm]	d_{iso} [ppm]	Ω *G98* [ppm]	Ω [ppm]	κ *G98*	κ
emim	−0.814	0.888	0.84	0.87	56.7	71.4	61.2	–	−0.45	–
	−2.572	0.808	0.69	0.93	93.7	91.7	67.8	–	−0.71	–
	−1.136	0.807	0.61	0.23	78.9	75	84.7	–	−0.03	–
	1.122	0.977	0.83	0.8	50.8	60.6	40.2	–	−0.26	–
bmim	−2.370	1.495	0.52	0.39	59.2	71.5	51.9	41.8	0.606	−0.448
	−2.835[a]	–	0.41[a]	–	56.3[a]	–	46.3[a]	–	0.465[a]	–
bdmim	1.336	0.978	0.92	0.11	63.7	71.6	71.4	77.7	−0.524	0.659
mbpyr	1.365	0.889	0.48	0.13	55.6	70.6	39.3	–	−0.311	–
	1.101	0.857	0.82	0.52	83.9	83.1	41.2	–	−0.468	–

[a] Monoclinic bmim values; not observed experimentally.

simulation of the NMR interaction tensors showed reasonable agreement with experimental findings.

The presence of order in halide ionic liquids persistent on the time scale of $\tau_c \sim 1/\omega_o$ were not observed in the liquid state as investigated experimentally by variable-temperature NMR spectroscopy. Relaxation time experiments showed that the liquid ILs studied have similar T_1 and T_2 relaxation constants near their melting points, demonstrating that they behave very much as typical liquids. A comparative study of spectra acquired at multiple field strengths revealed that residual second-order quadrupolar effects were absent, further demonstrating a lack of significant order on a timescale of $\sim 10^{-8}$ sec. The results suggest that reports in the literature of observed "structure" must exist on a shorter time scale as indeed evidence has been found for this by techniques such as FTIR, Raman spectroscopy and ab initio simulation and therefore are too short-lived to constitute "order" in molten ionic liquids on the timescales probed by herein.

To further explore this question it may be possible using NMR spectroscopy and isotopic labeling of the cations to evaluate any tendencies for the anions to remain associated with specific sites on the cation in the liquid state. The relative ease of synthesis of ionic liquids recommends this approach.

Experimental Section

All ionic liquids were supplied by EMD Chemicals except for bmim[Cl], which was supplied by Strem Chemicals and bNH_3[Br], which was made by standard metathesis techniques from *n*-butylbromide and an amine. All purchased samples were provided sealed under argon.

Sample Preparation: Samples were lightly ground, packed and sealed into sample tubes under argon since low concentrations of water can significantly alter RTIL properties.[27] bNH_3[Br] samples were synthesized and prepared in air and so it is important to note that there may be some water contamination in these samples; the extent of which was not characterized. Sample sizes included 4 mm outer diameter (o.d.) ceramic MAS rotors on the 900 MHz spectrometer, 7 mm o.d. ceramic MAS rotors on the 200 MHz, and 5 mm glass tubes cut to appropriate length for static spectra on the 400 MHz spectrometer. The following IUPAC-recommended chemical shift references were employed: 0.1 M solution of NaCl, a 0.01 M solution of NaBr, and 0.01 M solution of KI (all in D_2O) for chlorine, bromine, and iodine, respectively.[28] To establish "solid" central-transition, $\pi/2$ pulse lengths for solid IL samples, powdered and/or saturated solution samples of NaCl, KBr, NaBr, KI and NaI were used, as appropriate.

Differential Scanning Calorimetry: DSC analysis was used to establish parameters for VTNMR work. Rates used herein ranged from 1 to 5° min^{-1} as appropriate to the sample and practical considerations. Typically a sample was heated from room temperature past its melting point, resting isothermally for 10 min prior to cooling. Once past the freezing point (which was not always observed) another 10-minute isotherm was employed prior to execution of another heating ramp; this procedure determined the repeatability of thermal behaviour. Emphasis was placed on obtaining a reasonably accurate determination of the melting point of the sample in preparation for VTNMR studies; detailed studies of the thermal properties of ILs has been performed elsewhere with much greater attention paid to fine details.[29–31]

Experiments and Data Processing: NMR experiments were carried out with a Bruker AVANCE-II 900 MHz NMR spectrometer operating at a magnetic field of 21.1 T (Larmor frequencies: 88.19 MHz for ^{35}Cl, 225.52 MHz for ^{79}Br and 180.09 MHz for ^{127}I) using a standard-bore double-resonance 4 mm MAS NMR probe; a Tecmag 500 MHz NMR spectrometer operating at a magnetic field of 11.74 T (Larmor frequencies: 49.00 MHz for ^{35}Cl, 125.3 MHz for ^{79}Br and 100.06 MHz for ^{127}I) using a homemade standard-bore single-resonance 5 mm static NMR probe; a Bruker AVANCE 400 MHz NMR spectrometer operating at a magnetic field of 9.39 T (Larmor frequencies: 39.19 MHz for ^{35}Cl, 100.21 MHz for ^{79}Br and 80.03 MHz for ^{127}I) using a Morris Instruments wide-bore double-resonance 7 mm static NMR probe; and a Bruker AVANCE 200 MHz NMR spectrometer operating at a magnetic field of 4.7 T (Larmor frequencies: 19.60 MHz for ^{35}Cl, 50.12 MHz for ^{79}Br and 40.02 MHz for ^{127}I) using a Bruker wide-bore double-resonance 7 mm MAS NMR probe.

All MAS experiments were performed at ambient temperature. No corrections were made with respect to sample heating under MAS conditions; DSC experiments established with reasonable certainty that the heat generated would not have a significant impact on crystal structure. This assumption was borne out by correlation with static sample spectra; no changes in the quadrupolar tensor were observed. When necessary, the magic angle was set by standard procedure using the ^{79}Br signal from a solid powdered KBr sample: the angle is adjusted such that there are as many and as intensive rotational echoes as possible in the free induction decay (FID).

In all VTNMR experiments, the temperature was increased by 10 °C intervals to the desired temperature where it was allowed to sit for at least 10 min prior to initiating the pulse sequence. A thermocouple positioned close (within 1 cm) to the sample monitored the temperature; any deviation from the true sample temperature was considered insignificant. Heat was generated by a resistive coil under computer control and delivered by nitrogen gas flow to the sample stage area of the probe. Probe tuning and matching was performed at each temperature; significant drift was observed as the coil and capacitors in the resonance circuit were heated along with the sample.

The FIDs of the solid-state signals acquired herein were often quite short leading to a loss of information from the initial part of the fid during the ring-down time; to ensure that the experimental lineshapes would be relatively free of distortions, the spectra were acquired with Hahn Echo pulse sequences. Left-shifts were applied to ensure processing began at the top of the echo. Proton decoupling was used to improve the resolution of lineshape features. Please see Table 5 in the Supporting Information for pulse length details.

Spectrum simulations and fitting were carried out using the dmfit[12] and TopSpin programs. In dmfit simulations the "Q mas 1/2" model was used for MAS spectra and the Quasar[32] model was used for static spectra. Gaussian 98[33] was employed for ab initio calculations.

Acknowledgements

For access to the 900 MHz NMR spectrometer, we thank the National Ultrahigh Field NMR Facility for Solids (Ottawa, Canada), a national research facility funded by the Canada Foundation for

Innovation, the Ontario Innovation Trust, Recherche Québec, the National Research Council Canada, and Bruker BioSpin and managed by the University of Ottawa (www.nmr900.ca). The Natural Sciences and Engineering Research Council of Canada (NSERC) is acknowledged for a Major Resources Support grant. Carleton University is acknowledged for additional funding.

Keywords: chemical shifts · computational chemistry · ionic liquids · NMR spectroscopy · solid-state structures

[1] P. Walden, *Acad. Sci. St. Petersburg* **1914**, 405.
[2] S. M. Borisov, M. C. Waldhier, I. Klimant, O. S. Wolfbeis, *Chem. Mater.* **2007**, *19*, 6187.
[3] V. I. Pârvulescu, C. Hardacre, *Chem. Rev.* **2007**, *107*, 2615.
[4] F. van Rantwijk, R. A. Sheldon, *Chem. Rev.* **2007**, *107*, 2757 .
[5] V. L. Pushparaj, M. M. Shaijumon, A. Kumar, S. Murugesan, L. Ci, R. Vajtaj, R. J. Kinhardt, O. Nalamasu, P. M. Ajayan, *Proc. Natl. Acad. Sci. USA* **2007**, *104*, 13574.
[6] M. Sathish, K. Miyazawa, *J. Am. Chem. Soc.* **2007**, *129*, 13816.
[7] L. Xu, E. Choi, Y. Kwon, *Inorg. Chem.* **2007**, *46*, 10670.
[8] H. Weingärtner, *Angew. Chem.* **2008**, *120*, 664; *Angew. Chem. Int. Ed.* **2008**, *47*, 654.
[9] P. G. Gordon, D. H. Brouwer, J. A. Ripmeester, *J. Phys. Chem. A* **2008**, *112*, 12527.
[10] J. M. Aramini, H. J. Vogel, *J. Magn. Reson. Ser. B* **1996**, *110*, 182.
[11] M. Mehring, *Principles of High-Resolution NMR in Solids, 2nd ed.*, Springer, Berlin, **1983**.
[12] D. Massiot, F. Fayon, M. Capron, I. King, S. Le Calve, B. Alonso, J. O. Durand, B. Bujoli, Z. H. Gan, G. Haotson, *Magn. Reson. Chem.* **2002**, *40*, 70.
[13] C. J. Dymek, Jr., D. A. Grossie, A. V. Fratini, W. W. Adams, *J. Mol. Struct.* **1989**, *213*, 25.
[14] J. D. Holbrey, W. M. Reichert, M. Nieuwenhyuzen, S. Johnston, K. R. Seddon, R. D. Rogers, *Chem. Commun.* **2003**, 1636.
[15] P. Kölle, R. Dronskowski, *Inorg. Chem.* **2004**, *43*, 2803.
[16] S. Hayashi, R. Ozawa, H. Hamaguchi, *Chem. Lett.* **2003**, *32*, 498.
[17] H. Katayanagi, S. Hayashi, H. Hamaguchi, K. Nishikawa, *Chem. Phys. Lett.* **2004**, *392*, 460.
[18] J. A. Ripmeester, P. Gordon, G. Enright, S. Lang, *unpublished work*.
[19] R. P. Chapman, D. L. Bryce, *Phys. Chem. Chem. Phys.* **2007**, *9*, 6219.
[20] T. L. Weeding, W. S. Veeman, *J. Chem. Soc. Chem. Commun.* **1989**, 946.
[21] S. Hayashi, K. Hayamizu, *Bull. Chem. Soc. Jpn.* **1990**, *63*, 913.
[22] T. O. Sandland, L. Du, J. F. Stebbins, J. D. Webster, *Geochim. Cosmochim. Acta* **2004**, *68*, 5059.
[23] D. L. Bryce, M. Gee, R. E. Wasylishen, *J. Phys. Chem. A* **2001**, *105*, 10413.
[24] S. Tsuzuki, H. Tokuda, M. Mikami, *Phys. Chem. Chem. Phys.* **2007**, *9*, 4780.
[25] D. L. Bryce, G. D. Sward, *Magn. Reson. Chem.* **2006**, *44*, 409.
[26] S. Adiga, D. Aebi, D. L. Bryce, *Can. J. Chem.* **2007**, *85*, 496.
[27] J. A. Widegren, A. Laesecke, J. W. Magee, *Chem. Commun.* **2005**, 1610.
[28] R. Giernoth, D. Bankmann, *Prog. Nucl. Magn. Reson. Spectrosc.* **2007**, *51*, 63.
[29] K. Nishikawa, S. L. Wang, H. Katayanagi, S. Hayashi, H. O. Hamaguchi, Y. Koga, K. I. Tozaki, *J. Phys. Chem. B* **2007**, *111*, 4894.
[30] J. G. Huddleston, A. E. Visser, W. M. Reichert, H. D. Willauer, G. A. Broker, R. D. Rogers, *Green Chem.* **2001**, *3*, 156.
[31] H. L. Ngo, K. LeCompte, L. Hargens, A. B. McEwen, *Thermochim. Acta* **2000**, *357–358*, 97.
[32] J. Amoureux, *UCCS*, CNRS-8181, Lille, France, **2005**.
[33] M. J. Frisch, G. W. Trucks, H. B. Schlegel, G. E. Scuseria, M. A. Robb, J. R. Cheeseman, V. G. Zakrzewski, J. A. Montgomery Jr., R. E. Stratmann, J. C. Burant, S. Dapprich, J. M. Millam, A. D. Daniels, K. N. Kudin, M. C. Strain, O. Farkas, J. Tomasi, V. Barone, M. Cossi, R. Cammi, B. Mennucci, C. Pomelli, C. Adamo, S. Clifford, J. Ochterski, G. A. Petersson, P. Y. Ayala, Q. Cui, K. Morokuma, P. Salvador, J. J. Dannenberg, D. K. Malick, A. D. Rabuck, K. Raghavachari, J. B. Foresman, J. Cioslowski, J. V. Ortiz, A. G. Baboul, B. B. Stefanov, G. Liu, A. Liashenko, P. Piskorz, I. Komaromi, R. Gomperts, R. L. Martin, D. J. Fox, T. Keith, M. A. Al-Laham, C. Y. Peng, A. Nanayakkara, M. Challacombe, P. M. W. Gill, B. Johnson, W. Chen, M. W. Wong, J. L. Andres, C. Gonzalez, M. Head-Gordon, E. S. Replogle, J. A. Pople, *Gaussian 98 (Revision A.9)*, Gaussian, Inc., Pittsburgh PA, **2001**.

Received: August 6, 2009
Revised: October 10, 2009
Published online on November 18, 2009

